Supporting Information

Atomic-scale Structural and Chemical Characterization of Hexagonal Boron Nitride Layers Synthesized at the Wafer-Scale with Monolayer Thickness Control

Wei-Hsiang Lin[1], Victor W. Brar [1,2,3], Deep Jariwala[1,4], Michelle C. Sherrott[1,4], Wei-Shiuan Tseng[5], Chih-I Wu [6], Nai-Chang Yeh[2, 5], and Harry A. Atwater[1, 2,4*]

* haa@caltech.edu

1. Thomas J. Watson Laboratory of Applied Physics, California Institute of Technology, Pasadena, CA 91125, United States

2. Kavli Nanoscience Institute, California Institute of Technology, Pasadena, CA 91125, United States

3. Department of Physics, University of Wisconsin-Madison, Madison, WI 53711, United States

4. Resnick Sustainability Institute, California Institute of Technology, Pasadena, CA 91125, USA.

5. Department of Physics, California Institute of Technology, Pasadena, CA 91125, United States

6. Graduate Institute of Photonics and Optoelectronics and Department of Electrical Engineering, National Taiwan University, Taipei, Taiwan, Republic of China

Figure S1:

As shown in this figure S1 below, we can systematically vary the thickness of grown h-BN films from monolayer to 30 layers. We show the optical photograph and atomic force microscopy (AFM) analysis of these h-BN samples which have transferred onto 285nm SiO_2/Si substrates.

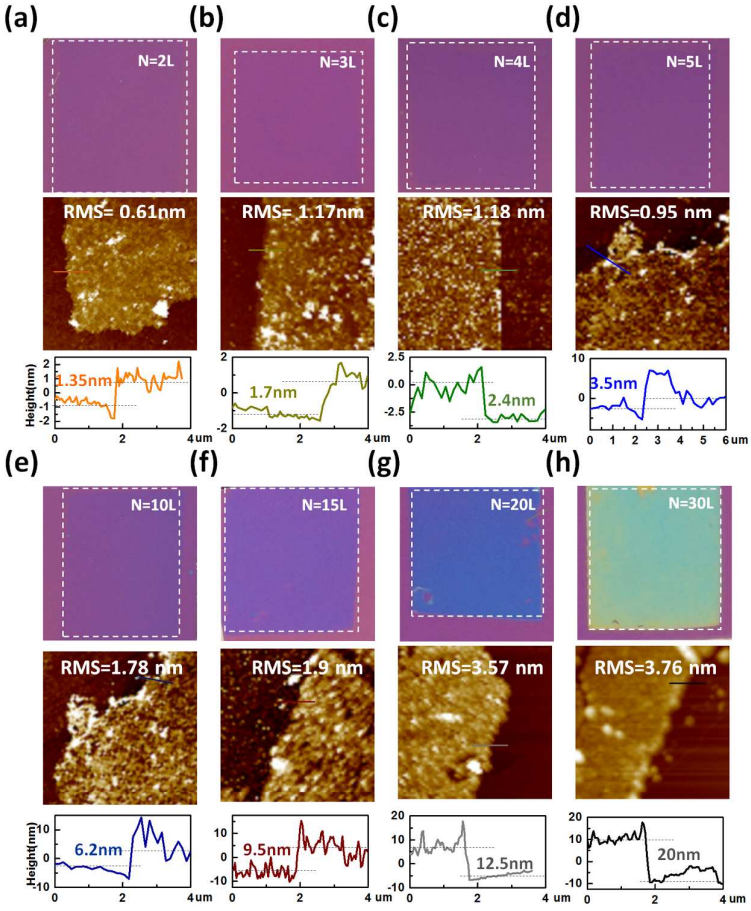

Figure S1: (a) - (d) Photograph of 2-layer h-BN to 5-layer thinner h-BN on SiO2/Si substrate within the white dash line and corresponding AFM images of bi-layer h-BN to 5-layer h-BN on SiO2/Si substrate and the height profile. (e) - (h) Photograph of thicker multi-layer h-BN (10 layers ~30layers) on SiO2/Si and corresponding substrate AFM images of multi-layer h-BN (10 layers ~30layers) on SiO2/Si substrate and the height profile.

Figure S2:

To further confirm the thickness dependence of these films we perform infrared transmission measurements using a Fourier transform infrared spectroscopy (FTIR) microscope as shown in Figure S2.

A typical infrared spectrum of an h-BN layer have two absorption bands at 1370 and 780 cm^{-1} correspond to transversal optical vibrations, respectively the in-plane B-N stretching mode(E_{1u}), and out of plane B-N-B bending mode (A_{2u}). For our normal incident experiment, infrared light should couple only with in-plane E_{1u} phonon mode. Figure S2a shows IR spectra of monolayer h-BN to 30 layers h-BN films, showing the $1\text{-}T/T_0$ was found to increase with the number of layers. Figure S2b suggests that the E_{1u} peak shift to higher energy as the film become thicker.

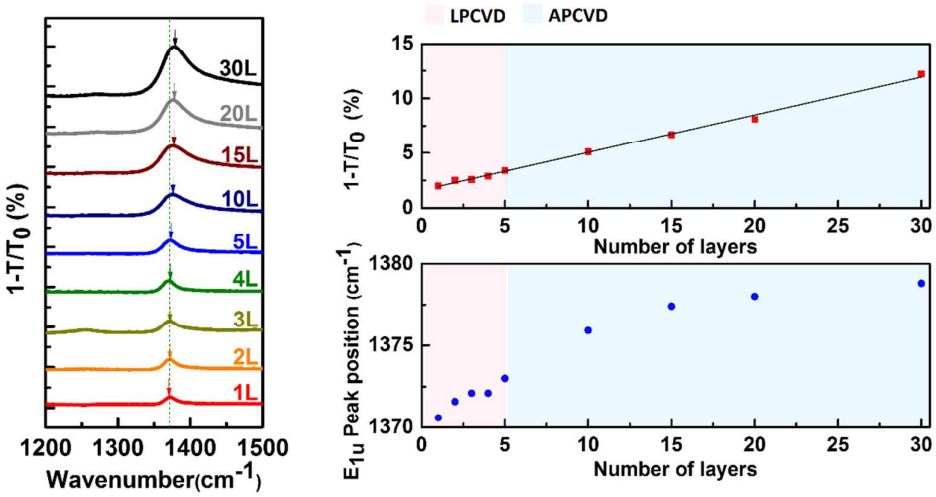

Figure S2: (Left) Infrared phonon of h-BN with the film thickness ranging from 30 layers to 1 layer. (Top right) The E_{1u} phonon intensity vs. number of monolayers of h-BN, showing the intensity increased with increasing the number of h-BN layers. (Bottom right) The E_{1u} phonon frequency increased with increasing the number of h-BN layers.

Figure S3:

We observe that the intensity of the Cu2p peak weakens with the increasing thickness of the h-BN films further corroborating our precise thickness controlled growth.

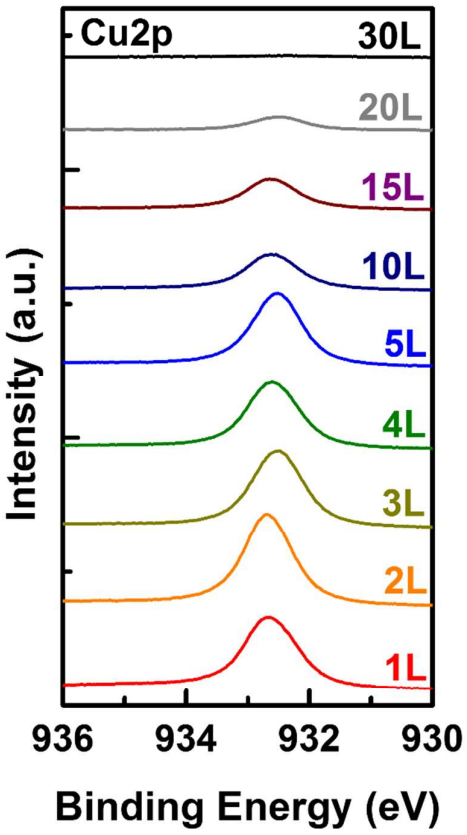

Figure S3: X-ray photoelectron spectra - Cu2p spectrum of 1 ~ 30 layers h-BN films on Cu foil used to identify the element present.

Figure S4:

For thicker (> 1 nm) h-BN films, we performed irreversible dielectric breakdown measurements to determine the hard-breakdown voltage.

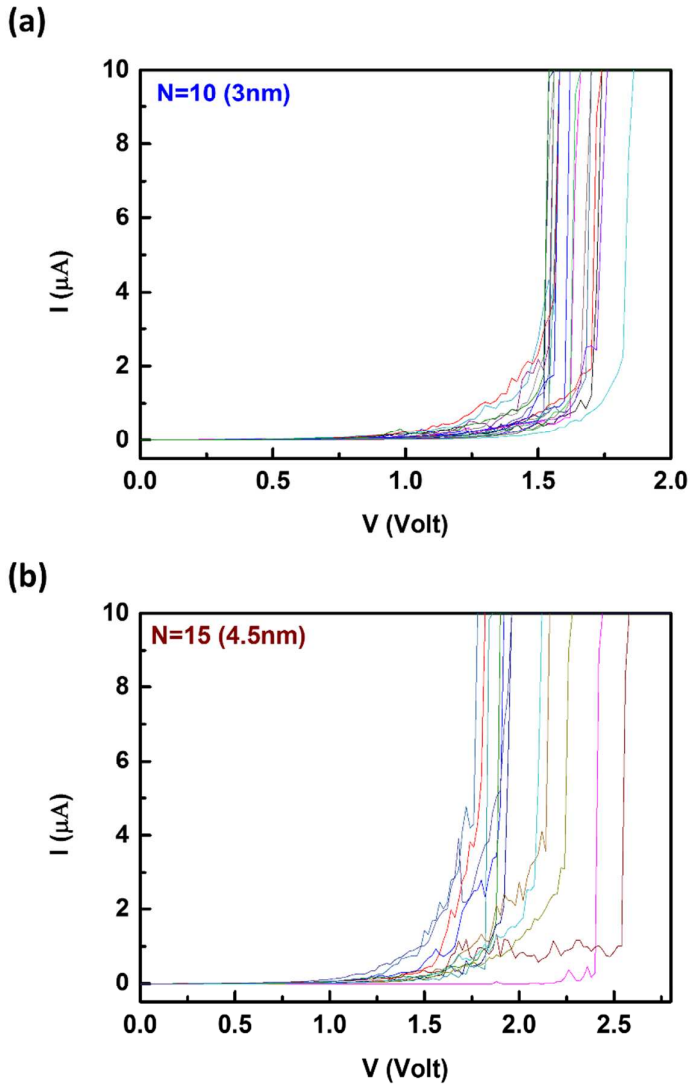

Figure S4: (a) The Characteristic I−V curves for Au / h-BN / Au devices with 3nm h-BN layer. (b) a) The Characteristic I−V curves for Au / h-BN / Au devices with 4.5nm h-BN layer

Figure S5:

As shown in figure S1 above, we can systematically vary the thickness of grown h-BN films by using a leak valve to control the flow rate of the borazine (or partial pressure of the borazine). In figure S5 below we show the quantitative dependence of h-BN film thickness on the partial pressure of the precursor (borazine). The growth temperature was fixed at 950ºC while the precursor temperature was fixed at 130ºC.

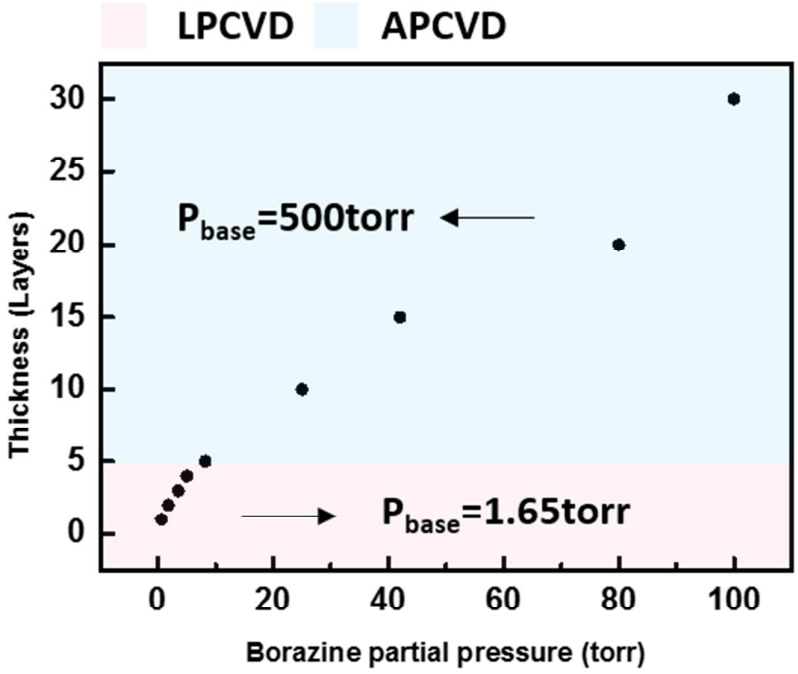

Figure S5. A plot of film thickness with respect to the Borazine partial pressure.

Figure S6:

In the previous report, Bhaviripudi *et al*. (Nano Lett. 2010, 10, 4128−4133.) elucidated the kinetic model for CVD synthesis of graphene. Similar to this report, figure S6 below depicts a steady state gas flow of a mixture of borazine, hydrogen, and argon gases on the surface of a Cu catalyst at a synthesis temperature (typically 950 °C). The main thermos-kinetics of the CVD process and reaction of borazine molecules include several steps:

The borazine species first (1) get transported to the reaction region, followed by (2) adsorption on Cu surfaces, (3) dehydrogenation of $B_3H_6N_3$ to form active boron and nitrogen species. Therefore, (4) surface diffusion of B and N species occurs on the Cu surface leading to, (5) growth of h-BN domains, and ultimately, (6) inactive species (such as hydrogen) diffuse away from the surface through the boundary layer. The above process can be classified into two regimes: mass transport region ($h_g \ll K_s$), primarily involving diffusion through the boundary layer, and surface reaction region (catalysis; $h_g \gg K_s$). In these growth regimes, the total pressure P_{TOT} determines whether boron nitride growth proceeded by catalysis or otherwise. For h-BN growths on Cu in LPCVD mode, we note that h_g increases as a result of lowering the total pressure which promotes surface catalysis ($h_g \gg K_s$), tending to grow from monolayer to thin multi-layer h-BN. In APCVD growth conditions, we note an increase in surface growth rate K_s and decrease in mass transfer coefficient h_g which makes the mass transport flux dominant over surface reactions ($h_g \ll K_s$). This means the h-BN growth will continue to happen until elimination of all the high temperature pyrolyzed species of ammonia-borane which ultimately leads to growth of thick multilayer h-BN without the need of surface catalysis of Cu.

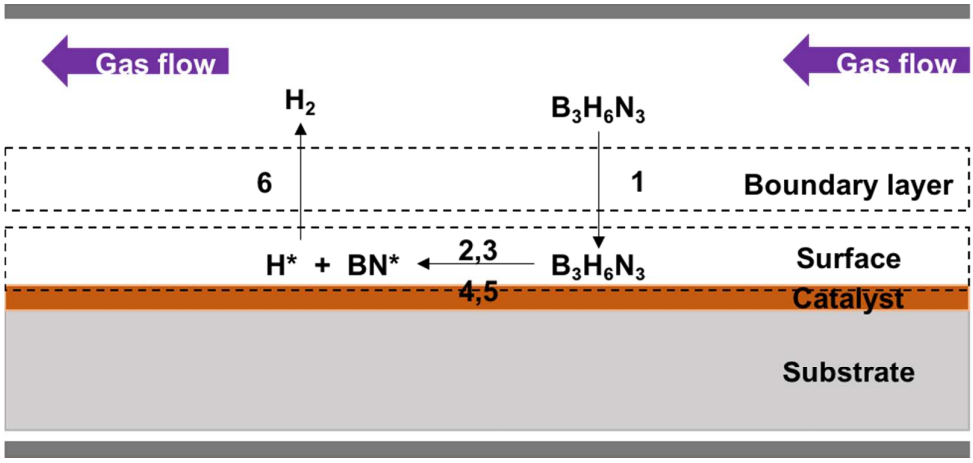

Figure S6. Processes involved during h-BN synthesis on Cu in a CVD process

Figure S7:

To estimate the domain size in our CVD grown h-BN films we perform scanning electron microscopy of sub-monolayer growth directly on the copper substrate. A sub-monolayer growth would provide strong contrast in the SEM between the insulating h-BN and conductive copper foil. Figure S7 below shows some SEM micrographs of sub monolayer growths and analysis of domain sizes.

Figure S7 (a) shows large scale SEM image with different h-BN domain sizes. The sharp geometric and triangular edge features suggests the highly crystalline nature of the growth as verified by STM, TEM and Raman in the manuscript. Figure S7 (b) and (c) shows the higher magnification images of triangular h-BN domains with edge length of ~500nm and ~1 μ m respectively. The statistical distribution of domain size is plotted Figure S7 (d) which shows that the average domain size of h-BN is ~750nm.

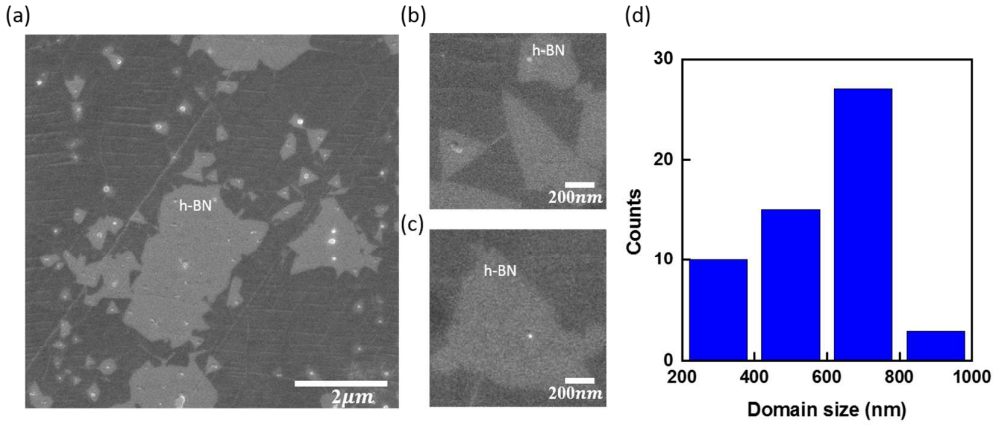

Figure S7. (a)-(c) SEM images showing triangular ad-layer with different domain size. (d) Histograms for the h-BN domain size.

Figure S8:

To provide further evidence of the thickness of our growth h-BN film we perform high resolution transmission electron microscopy of the same film samples that were characterized using AFM. We took one 5 layers h-BN sample which is defined by our AFM measurement (Supplementary information S1) and transferred on TEM grids. Here, we show a cross-section TEM with 5 fringes which is consistent with our thickness of ~3.5nm determined by AFM measurements.

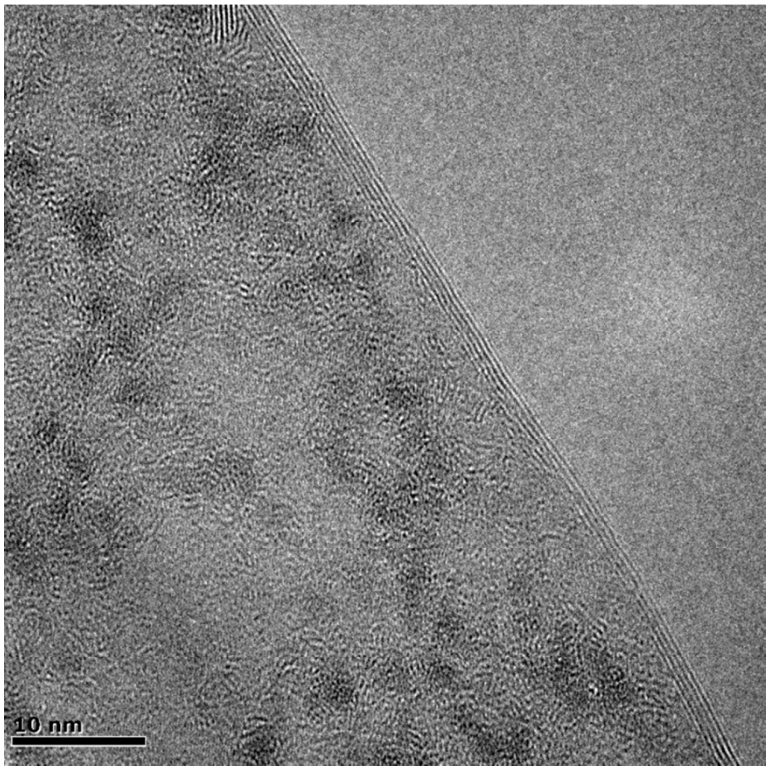

Figure S8. Cross – section TEM image of 5-layer h-BN.

Figure S9:

A representative atomic force microscopy (AFM) image below shows a large scale $40\mu m \times 40\mu m$ topography image of 5-layer h-BN sample to show the thickness uniformity of the film. This h-BN film was grown on Cu and transferred onto 285nm SiO_2/Si substrate. The root mean square roughness extracted from this AFM micrograph is 0.69nm.

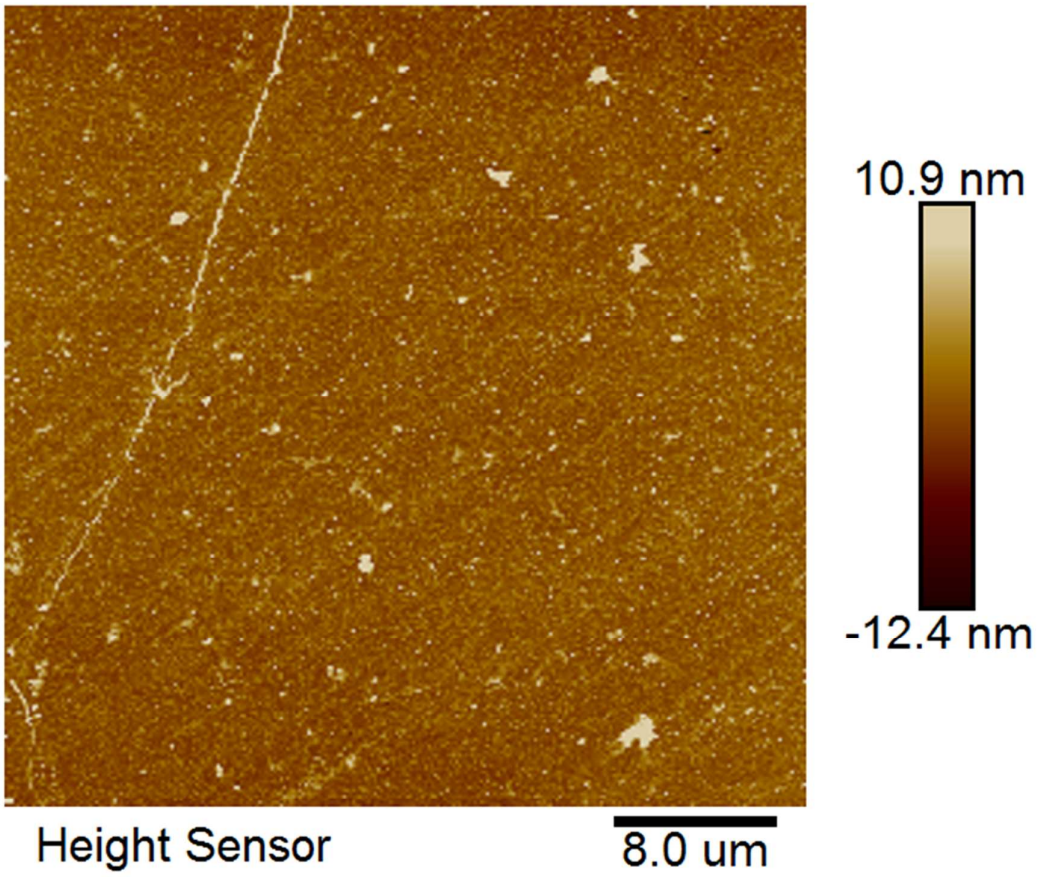

Figure S9. AFM image of 5-layer h-BN.